

RESEARCH NOTE

Fabrication of Ir/TiO₂(110) Planar Catalysts with Tailored Particle Size and Distribution

A. Berkó, G. Klivényi, and F. Solymosi

Reaction Kinetics Research Group, Hungarian Academy of Sciences, Hungary, and Institute of Solid State and Radiochemistry, Attila József University, P.O. Box 168, H-6701, Szeged, Hungary

Received August 21, 1998; revised September 16, 1998; accepted November 4, 1998

A simple method is described by which supported Ir nanoparticles can be fabricated in desired uniform sizes in the range of 1.5–20.0 nm with constant interparticle distances. The nanoparticles are characterized by STM. The method exploits the significant differences in the diffusion rates of metal adatoms and nanocrystallites, and consists of two steps: (i) vapor deposition of Ir metal in predetermined concentrations on titania at 300 K with a postannealing at 1200 K, and (ii) subsequent evaporation of Ir on this surface at 1200 K.

© 1999 Academic Press

INTRODUCTION

There is increasing evidence that the rate and the direction of several catalytic reactions depend on the size of catalyst particles (1). The classic impregnating technique generally produces metal crystallites in a broad particle size distribution, and the distance between metal particles is not controlled. This makes it very difficult to study the size dependence of crystallites on its catalytic performance. Several new techniques have been developed to produce particles with very narrow size distribution (2–12). Most of these methods, however, cannot fulfill all the requirements, i.e., uniform size, regular spatial distribution, and sufficient number of metal clusters.

One of the new methods, called pulsed laser deposition (PLD), produced small particles, but sizes varied in the range of 2–50 nm, and the particle distances also were not controlled (3–5). Another promising technique also applied in this area is electron beam lithography (EBL), which provides the fabrication of a square array of metal particles on oxidic support (6–12). The method consists of several steps, including spin coating of an electron-sensitive polymer, bombardment of the polymers with a highly collimated electron beam, selective dissolution of the polymer damaged by electron exposure, evaporation of metals on the sample, and removal of the remaining resistant polymer by dissolution. The Pt array thus pre-

pared contains an overlayer of carbonaceous material, which can be removed by cycles of bombardment with neon ions followed by annealing at 550–600 K. In this way it was possible to produce platinum particles of 25–50 nm diameter and 15 nm height at 200 nm spacing on an oxidized silicon wafer (9–12). The size of the crystallites is primarily controlled by the size of the holes created by the electron beam. This crystallite is quite large: high reactivity of metal clusters is exhibited at much smaller nanoparticles, and crystallites larger than 20–25 nm generally show no size dependence at all. This was well demonstrated in the case of the interaction of CO with Rh nanocrystallites (13–16). Whereas Rh particles of 2–4 nm size disrupted almost instantaneously into smaller units, and finally atomically dispersed Rh, this process was not observed by STM for particles larger than 10–15 nm. The same feature was observed for the supported Ir nanocluster (17).

Nanoparticles with a predetermined distribution can also be produced by ordered nucleation of the particles where the thermodynamic properties of the surface diffusion processes are exploited. For this propose faceted or reconstructed substrates are the favorites because the demand for inhomogeneous and/or anisotropic surface diffusion properties is usually fulfilled (18).

In this work we describe a preparation of Ir nanoparticles from 2–3 nm up to giant (20–30 nm) Ir crystallites with rather uniform sizes and controlled spatial distribution. This method is based on our recent finding that there is a large difference in the diffusion of Rh adatoms and Rh nanocrystallites on oxidic supports (19).

EXPERIMENTAL

The experiments were carried out in a UHV chamber equipped with a three-grid AES-LEED analyzer and a commercial STM head purchased from WA Technology. The homemade evaporator was a liquid nitrogen-cooled and thermally heated construction. During the Ir dosing

the distance between the evaporator surface and the sample was approximately 20 mm. The rate of the deposition was controlled by adjusting the current flowing through the Ir filament spot welded to a thicker W rod. The amount and the purity of the epitaxial Ir layer on the titania were checked by AES spectroscopy. The surface concentration of the deposited metal is given in monolayer equivalent (ML), which corresponds to 1.5×10^{15} Ir atoms/cm². The calculation of this value is based on the apparent volume of 3D metal crystallites observed on STM images at metal coverage around 1 ML (17, 19–21). The deposition rate of Ir was always less than 1 ML/10 min. It is important to note that the formation of crystallite seeds increases substantially at higher deposition rates.

The polished TiO₂(110) single crystal sample was purchased from Crystal-Tec. Without any further treatment in air it was clipped with a Ta plate on a transferable sample holder and moved into the chamber. The sample was heated by a W filament positioned just below the Ta plate carrying the probe. The cleaning procedure of the TiO₂ has been described in our previous paper (22). In this work we also observed that annealing of the cleaned sample at 800–900 K resulted in a mainly bulk-terminated 1×1 surface. Highly ordered 1×2 reconstructed terraces covering 80–90% of the total area could be obtained only after annealing at 1200 K in UHV. The characteristic morphology of TiO₂(110)-(1×2) is described and discussed in detail in several recent papers (22–25). The STM pictures show characteristic step lines in the direction of [001], $[\bar{1}13]$, and $[1\bar{1}1]$ and well-ordered (1×2) reconstructed terraces with an average size of (20 nm)².

RESULTS AND DISCUSSION

The fabrication of Ir clusters in a predetermined size and spatial distribution consists basically of two steps. (i) A predetermined concentration of Ir is deposited on TiO₂ at room temperature and annealed at 1200 K. This first step is called “seeding.” The number of Ir clusters thus produced primarily depends on the amount of Ir deposited on the titania at 300 K. (ii) The subsequent evaporation of Ir onto this surface at 1200 K, which leaves the particle density of the Ir nanoparticles practically unchanged, causes the growing of Ir crystallites. This second step of the treatment is called “growing.”

In order to demonstrate the efficiency of this method, we performed three series of measurements. In the first case a very small amount of Ir (0.003 monolayer, ML) was deposited on TiO₂(110)-(1×2) at 300 K, and then the sample was heated for 10 min at 1200 K (Fig. 1A). The resulting Ir adparticles were of 1.5 nm size, which contains about 10–20 Ir atoms. The average distance between the particles is 40 nm (Fig. 1A). The growing of these particles by the increased deposition of Ir at 1200 K is presented in

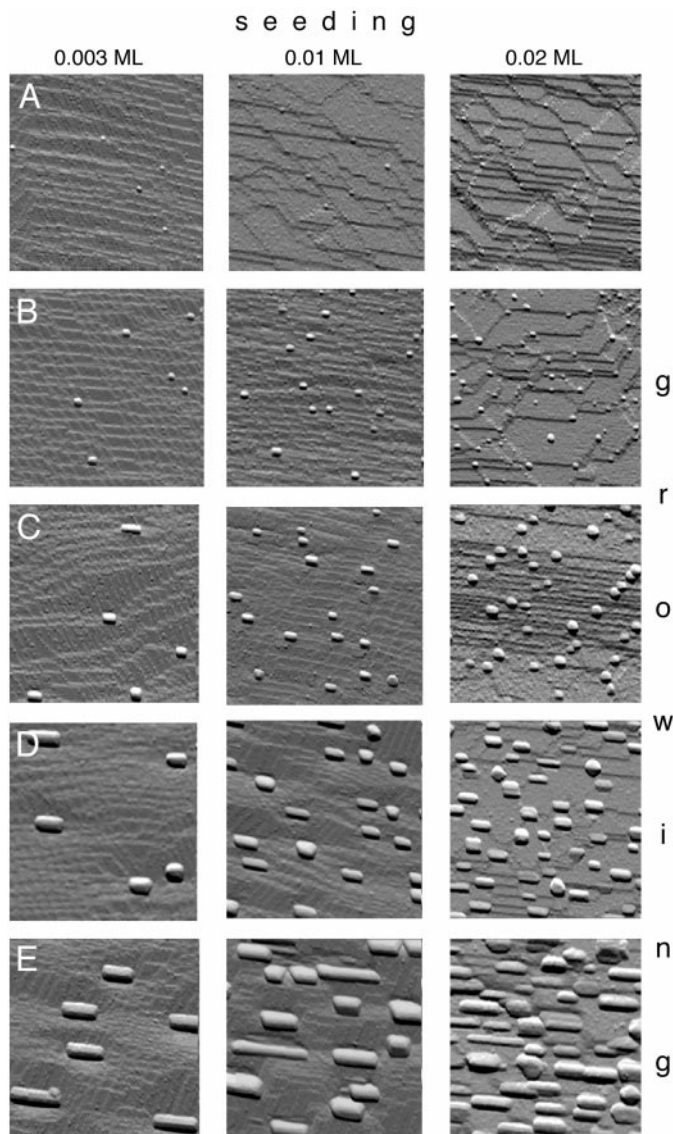


FIG. 1. STM images of the Ir particles grown on TiO₂(110)-(1×2) by the predeposition of different amounts of iridium at 300 K followed by annealing at 1200 K in UHV: (A) 0.003, 0.01, and 0.02 ML of Ir. (B–E) Growing of the Ir crystallites by postdeposition of increasing amount of iridium at 1200 K. The image size is 100 nm \times 100 nm in all cases.

Figs. 1B–E. An important feature of the pictures is that the size of the Ir particles is uniform and the spatial distribution remains the same. The shape of the clusters is strongly elongated in the crystallographic orientation of [001], when the particle size reaches a critical value of approximately 4 nm. This behaviour clearly refers to crystallization coordinated by the row structure of the support and also suggests that the diffusion coefficient is strongly anisotropic due to the anisotropic structure of the TiO₂(110)-(1×2) surface. This observation is in agreement with the strong site preference of the small particles mentioned above. The height of the largest crystallites falls in the range of 1.0–1.5 nm, which

TABLE 1
Characteristic Data for the Ir Particles

Image on Fig. 1	Admetal coverage (ML)	Number of the particles per (100 nm) ²	Average diameter (nm) ^a	Standard deviation (nm)	Average height (nm)	Standard deviation (nm)	Average interparticle distance (nm)
Seeded by 0.003 ML							
A	0.003	5	1.5	±0.1	0.30	±0.1	
B	0.015	6	3.5	±0.3	0.65	±0.1	
C	0.04	5	4.5	±0.6	0.95	±0.1	40
D	0.10	5	8.0	±1.0	1.15	±0.2	
E	0.40	6	11.0	±1.4	1.30	±0.2	
Seeded by 0.01 ML							
A	0.01	17	1.5	±0.1	0.35	±0.1	
B	0.03	19	3.0	±0.3	0.60	±0.1	
C	0.10	18	4.5	±0.7	0.75	±0.2	27
D	0.52	20	6.5	±1.1	1.25	±0.2	
E	1.70	17	13.0	±1.6	1.60	±0.3	
Seeded by 0.02 ML							
A	0.02	48	1.5	±0.1	0.30	±0.1	
B	0.05	46	3.0	±0.2	0.50	±0.1	
C	0.20	42	5.0	±0.6	0.70	±0.2	13
D	1.30	51	7.0	±1.1	1.05	±0.3	
E	2.50	44	12.0	±2.2	1.35	±0.3	

^a In the case of elongated particles the approximation of diameter = $\sqrt{4 \times \text{length} \times \text{width}/\pi}$ was used.

means that they consisted of approximately 4–6 atomic layers. Unfortunately, it is difficult to determine the inner structure of the crystallites from our experiments. The fact that clusters smaller than 3–4 nm never show elongated geometry may indicate that the smaller particles are strongly influenced by the microscopic corrugation of the substrate, preventing the ordering of their crystal lattice. Nevertheless, the hexagonal outline of larger particles clearly suggests that their top facet is the (111)-oriented plane. The strongly elongated crystallites may possess another inner structure, probably (100) top face.

Similar features were observed when the initial density of Ir clusters was increased by seeding of 0.01 and 0.02 ML of Ir (Fig. 1). The characteristic data for the Ir particles prepared in this way (average size, density) are collected in Table 1. It appears that by the variation of the predeposited Ir in the range of 0.003–0.05 ML the average particle density (or in other words the separation) can be finely adjusted in the range of 1–100 particles per (100 nm)² surface area (10¹⁰–10¹² particles/cm²) without a strong effect on the average size of the particles (typically 1–2 nm). By the second step, the average size of the particles can be increased at will up to 15–20 nm, without the alteration of the average distance between the clusters. The local morphology of the substrate (step, terrace distribution) has only a slight modification effect on the particle distribution; namely, the local particle density is larger on a region where the step density is higher. This fact strongly suggests that the systematic modification of the surface (i.e., faceting by misalignment) means a

further new chance for tailoring of the particle distribution.

CONCLUSIONS

A new method consisting of “seeding + growing” procedures is suitable for fabricating supported metal clusters in desired sizes between 1.5 and 20 nm and density in the range of 1–100 particles over (100 nm)². The advantage of this method in comparison to lithography is the former’s relative simplicity and the possibility of preparing nanoparticles in a much smaller size.

ACKNOWLEDGMENTS

This work was supported by the Hungarian Academy of Sciences and by OTKA14889.

REFERENCES

- Fendler, J. H., and Dékány, I. (Eds.), “Nanoparticles in Solids and Solutions.” Kluwer Academic, Dordrecht/Norwell, MA, 1996.
- Gunter, P. L. J., Niemantsverdriet, J. W., Riberio, F. H., and Somorjai, G., *Catal. Rev.* **39**, 77 (1997).
- Eppler, A. S., Rupprechter, G., Guzzi, L., and Somorjai, G. A., *J. Phys. Chem. B* **101**, 9973 (1997).
- Foltyn, S. R., in “Laser Ablation for Materials Synthesis” (D. A. Payne and J. C. Bravman, Eds.), p. 205. Mater. Res. Soc. Symp. Proc., Vol. 191. 1990.
- Pászti, Z., Pető, G., Horváth, Z. E., Karacs, A., and Guzzi, L., *J. Phys. Chem. B* **101**, 2109 (1997).
- Cerrina, F., and Marrian, C., *MRS Bull.* **21**, 56 (1996).

7. Wong, K., Johansson, S., and Kasemo, B., *Faraday Discuss.* **105**, 237 (1996).
8. Fischer, P. B., and Chou, S. Y., *Appl. Phys. Lett.* **62**, 2989 (1993).
9. Jacobs, P. W., Riberio, F. H., Somorjai, G. A., and Wind, S., *Catal. Lett.* **37**, 131 (1996).
10. Jacobs, P. W., Wind, S., Riberio, F. H., and Somorjai, G. A., *Surf. Sci.* **372**, L249 (1997).
11. Somorjai, G. A., *Appl. Surf. Sci.* **121**, 1 (1998).
12. Eppler, A. S., Rupprechter, G., and Somorjai, G. A., to be published.
13. Solymosi, F., and Pásztor, M., *J. Phys. Chem.* **89**, 4789 (1985).
14. Solymosi, F., and Pásztor, M., *J. Phys. Chem.* **90**, 5312 (1986).
15. Solymosi, F., and Bánsági, T., *J. Phys. Chem.* **97**, 10133 (1993), and references therein.
16. Berkó, A., Ménesi, G., and Solymosi, F., *J. Phys. Chem.* **100**, 17732 (1996).
17. Berkó, A., and Solymosi, F., *Surf. Sci.* **411**, 1900 (1998).
18. Francis, G. M., Kuipers, L., Cleaver, J. R. A., and Palmer, R. E., *J. Appl. Phys.* **79**, 2942 (1996).
19. Berkó, A., and Solymosi, F., *Surf. Sci.* **400**, 281 (1998).
20. Poirier, G. E., Hance, B. K., and White, J. M., *J. Vac. Sci. Technol. B* **10**, 6 (1992).
21. Berkó, A., Ménesi, G., and Solymosi, F., *Surf. Sci.* **372**, 202 (1997).
22. Berkó, A., and Solymosi, F., *Langmuir* **12**, 1257 (1996).
23. Fischer, S., Munz, A. W., Schierbraun, K.-D., and Göpel, W., *Surf. Sci.* **337**, 17 (1995).
24. Cocks, I. D., Guo, Q., Patel, R., Williams, E. M., Roman, E., and DeSegovia, J. L., *Surf. Sci.* **377**, 135 (1997).
25. Guo, Q., Cocks, I. D., and Williams, E. M., *Phys. Rev. Lett.* **77**, 3851 (1996).